Direct Observation and Measurements of Neutron Induced Deep Levels Responsible for N_{eff} Changes in High resistivity Silicon Detectors Using TCT*

Z. Li and C.J. Li+
Brookhaven National Laboratory,
Upton, New York 11973, USA

V. Eremin, and E. Verbitskaya
Ioffe Physico-Technical Institute, Russian Academy of Sciences,
194021 St-Petersburg, Russia

+ Permanent Address: Institute of Semiconductors, Chinese Academy of Sciences, Beijing, 100083, China

Abstract

Neutron induced deep levels responsible for changes of space charge concentration N_{eff} in high resistivity silicon detectors have been observed directly using the transient current technique (TCT). It has been observed by TCT that the absolute value and sign of N_{eff} experience changes due to the trapping of non-equilibrium free carriers generated near the surface (about 5 m depth into the silicon) by short wavelength laser pulses in fully depleted detectors. Electron trapping causes N_{eff} to change toward negative direction (or more acceptor-like space charges) and hole trapping causes N_{eff} to change toward positive direction (or more donor-like space charges). The specific temperature associated with these N_{eff} changes are those of the frozen-up temperatures for carrier emission of the corresponding deep levels. The carrier capture cross sections of various deep levels have been measured directly using different free carrier injection schemes.

I. INTRODUCTION

The transient current technique (TCT) has been applied quite successfully for the investigation on irradiated high resistivity silicon detectors in recent years. Some examples of the TCT successes are: 1) detector internal electric field profiling [1-2]; 2)Fermi level positioning [3]; 3) N_{eff} (space charge concentration) determination [3-4]; 4) carrier drift mobility study [5]; and 5) study of electric field transformation [6]. In this paper, we present a novel approach for the measurements of defect levels in the silicon energy band gap using TCT. This work is the extension of the study carried out in ref. [6] in which the effect of trapping induced N_{eff} (or field) transformation in irradiated high resistivity silicon detectors was first discovered. Since the trap levels measured by the TCT method are directed related to the

N_{eff} changes (or transformations), this is the first time one observes and measures directly the deep levels responsible for the N_{eff} changes (denoted here as N_{eff} defects for simplicity). The TCT method therefore does not need to correlate to other measurements of N_{eff} (as is the case for deep level transient spectroscopy (DLTS) and thermally stimulated current (TSC)) and is therefore superior method in determining N_{eff} defects.

II. SAMPLES AND EXPERIMENTAL TECHNIQUE

Silicon $p^+/n/n^+$ junction detectors were produced from n-Si with resistivity of 2-4 kΩ-cm and 4-6 kΩ-cm. The detector thickness is ranging from 290 μm to 630 μm and p^+-contact area is 0.25 cm^2. The p^+-contact was formed by boron implantation into a window in the SiO_2 layer in the front side of the wafer. The n^+-contact was formed by phosphorus implantation over the entire back side of the wafer (with SiO_2 layer etched off). Metallization contacts were made by depositing Al over the window area for the front side (p^+) and over the entire wafer for the back side (n^+). For detector light sensitivity, a hole of 2 mm diameter was etched on Al layers on both p^+ and n^+ contacts for each detector.

Detectors were irradiated by 1 MeV neutrons at the University of Massachusetts at Lowell in the fluence range of $2x10^{12}$ to $10x10^{12}$ n/cm^2. The Brookhaven National Lab's (BNL) TCT system, as shown in Fig. 1, utilizes a semiconductor pulsed laser diode with wavelength of 670 nm that allows the generation of electron hole pairs adjacent to the contact (about 3-5 μm beneath the contact), a cryostat for cooling detectors in the temperature range of 77-300 K, and a sampling oscilloscope (TDS-744) to record the induced current shapes. Since the laser absorption length is only about 1% or less of the detector thickness, the induced current shapes can be considered as being generated by a two dimensional, one-type of carrier (electron or hole) charge layer. This assumption makes it possible to obtain dimensional, analytical simulations.

III. Theoretical Considerations

For a two dimensional charge layer with only one type of carriers contributing to the induced current shape, it can be simulated by the following one dimensional model:

$$\begin{cases} i(t,T) = Q_0 \cdot E_w \cdot v_d(t,T) = \dfrac{Q_0}{d} \cdot v_d(t,T) \\ v_d(t,T) = \dfrac{dx}{dt} = \dfrac{\mu_0(T) \cdot E(x)}{1 + \mu_0(T) \cdot E(x) / v_s} \\ q(t) = Q_0 \ \ at \ \ (x = 0, t = 0) \\ x = 0 \quad at \ \ t = 0 \end{cases} \tag{1}$$

where $i(t,T)$ is the induced current at time t and temperature T, Q_0 the total charge (one type) generated by laser, E_w the waiting field, $v_d(t,T)$ the carrier drift velocity, d the detector thickness, x the location of the drifting charge layer, $\mu_0(T)$ the carrier low field drift mobility which can be for either electrons ($\mu_0^e(T)$) or holes ($\mu_0^h(T)$), v_s the carrier saturation velocity, and $E(x)$ the electric field in the detector. In the case positive space charge (junction on the p^+ side or junction front, JF), as shown in Fig. 2a, $E(x)$ can be expressed as:

$$\begin{cases} E(x) = E_0 \cdot (1 - \dfrac{x}{d}) + E_d \\ E_0 = \dfrac{eN_{eff} \cdot d}{\varepsilon\varepsilon_0} \ , \ E_d = \dfrac{V - V_d}{d} \end{cases} \tag{2}$$

From eq. (1) and (2) one can solve the location x of the drifting electron charge layer (laser on the front side, LF) as a function of time t:

$$t = \frac{x}{v_s} + \tau \cdot \ln\left[\frac{E_0 + E_d}{E_0(1 - \frac{x}{d}) + E_d}\right] \ , \ \tau = \frac{\varepsilon\varepsilon_0}{e\mu_0^e(T) \cdot N_{eff}} \qquad \text{(JFLF)} \qquad (3)$$

Similarly, in the case negative space charge (junction on the n^+ side or junction back, JB), as shown in Fig. 2b, the location x of the drifting electron charge layer as a function of time t can be expressed as:

$$t = \frac{x}{v_s} + \tau \cdot \ln\left[\frac{E_0 \cdot \frac{x}{d} + E_d}{E_d}\right] \ , \ \tau = \frac{\varepsilon\varepsilon_0}{e\mu_0^e(T) \cdot N_{eff}} \qquad \text{(JBLF)} \qquad (4)$$

The carrier drift velocity can be calculated using $v_d=dx/dt$ and the drift current $i(t,T)$ can be then calculated using eq. (1).

It is easy to prove [7] that, for the case of drifting hole current (junction back at $x=d$, laser back at $x=d$ (JBLB); and junction front at $x=0$, laser back at $x=d$ (JFLB)), one can simply make the following transformations:

$$\mu_0^e(T) \rightarrow \mu_0^h(T) \text{ and } x \rightarrow d\text{-}x \qquad (5)$$

in eq. (3) for JBLB and eq.(4) for JFLB.

For the complete simulation, one needs the dependence of carrier drift mobility on temperature. We will use the data (Table I) from our early carrier drift mobility study [5], which has shown that there was no degradation of the carrier drift mobility in detectors irradiated to less than $1\text{x}10^{14}$ n/cm^2. The average saturation velocities obtained from ref. [5] are also listed in Table I, which are temperature independent.

Fig. 3a shows the simulated hole current shapes (LB) with various N_{eff} values (negative space charge, or JB). The biases were chosen such that the over-depletion voltage (V-V_d) was fixed at 50 volts. It is clear that the average slope (S) of the current shape top increases with the value of N_{eff}. In fact it is clearly shown in Fig. 3b that S is nearly proportional to N_{eff} at a given temperature T. However, due to the dependence of τ on the drift mobility $\mu_0(T)$ (eq. (3) and (4)), the value of S changes with T for a given N_{eff}. Fig. 4a shows the temperature dependence of S for electron current and Fig. 4b shows that for hole current. It is clear that this dependence is not linear. However, we may approximate this dependence as a simple two-stage dependence of T to a constant power. With these approximations, one can relate the average top slope S to the value of N_{eff} as the following:

$$N_{eff} = -\frac{S \cdot d}{Q_0 / e} \cdot \begin{cases} 1.5117 \times 10^{16} \cdot \left(\frac{T}{300}\right)^{3.6698} & (T > 237\ \text{K}) \\ 6.2046 \times 10^{15} \cdot \left(\frac{T}{300}\right)^{-0.2599} & (T \le 237\ \text{K}) \end{cases} \quad (\text{cm}^{-3}) \text{ (for electron current)} \quad (6)$$

$$N_{eff} = \frac{S \cdot d}{Q_0 / e} \cdot \begin{cases} 8.1800 \times 10^{16} \cdot \left(\frac{T}{300}\right)^{3.5663} & (T > 192\ \mathrm{K}) \\ 1.7392 \times 10^{16} \cdot \left(\frac{T}{300}\right)^{0.1009} & (T \le 192\ \mathrm{K}) \end{cases} \quad (\mathrm{cm}^{-3}) \text{ (for hole current)} \qquad (7)$$

Note here that the signs for both S and N_{eff} have been incorporated in eq. (6) and (7). A negative value of S means a current decay (carriers moving from high field to low field) and a positive value means a current increase (carriers moving from low field to high field). While the sign of N_{eff} represents the sign of the space charge.

It is necessary to point out that the effect of carrier trapping by deep levels was not explicitly expressed in eq. (6) and (7). However, due to the combination effect of free carrier trapping with trapping time constant:

$\tau_t = [\sigma \cdot \upsilon \cdot n_0]^{-1}$ (n_0: the average injected free carrier density) (8)

and different degree of freezing-out of detrapping at different temperatures with detrapping time constant:

$$\tau_d = [\sigma \cdot \upsilon \cdot N_{C,V} \cdot e^{-\frac{E_a}{kT}}]^{-1} \qquad (9)$$

of deep levels, the value and the sign of the charge state density N_{eff} may change [6] In eq. (8) and (9), σ_t is the defect carrier capture cross section, v_{th} the carrier thermal velocity, $N_{C,V}$ the density of states, and E_a the defect activation energy. This makes the steady-state measurement (measurement time τ_m satisfies: $\tau_t << \tau_m << \tau_d$) of the current shape top slope S as a function of T a direct measurement of N_{eff} defects. The characteristic temperature T_c for each N_{eff} defect at which the value and/or sign of N_{eff} undergoes a transformation is the freezing-out temperature of this defect (no detrapping). The relationship between the defect activation energy E_a and T_c is similar to that in a TSC measurement since the time constants of both measurements are similar (in the order or 10's of seconds for each defect level) [8].

IV EXPERIMENTAL RESULTS AND DISCUSSIONS

Fig. 5 shows the laser induced steady-state current shapes (measured at 100 Hz repetition rate from high temperature to low temperature with temperature stabilization time of about 10 sec) at 70 volts and various temperatures for an un-irradiated detector. It is clear that current shape top slope S does not change sign for both electron injection (Fig. 5a) and hole injection (Fig. 5b). Some increases of S in both cases with decreasing temperature are caused by the mobility effect ($\mu_0(T)$ through τ, see eq. (3)), which can be corrected by eq. (6) and (7). Mobility temperature dependence also affects the width of the current shape which is a measure of the average carrier drift velocity [5].

The laser induced steady-state electron shapes at 100 volts and various temperatures for a detector irradiated to $2.3\text{x}10^{12}$ n/cm^2 are shown in Fig. 6. The sign of the space charge (or N_{eff}) is positive at 300 K, indicating that the junction is on the p^+ side. At around 150 K, the sign of space charge transforms from positive to negative, denoted here as SCT(+,-), due to the trapping of the drifting electrons and subsequent freezing-out at neutron irradiation induced deep trap levels. The junction therefore shifts from its position near the p^+ side at 300 K to that near the n^+ side at below 150 K. This SCT(+,-) in a conventional term would mean "type inversion" near T=150 K. At temperatures lower than 150 K, the absolute value of N_{eff} becomes so large that a given bias can no longer deplete the detector. This is evident from the appearance of a long tail (diffusion) and eventual degradation of current shapes or charge collection, which are caused by partial depletion [6].

For $p^+/n/n^+$ junction detectors irradiated beyond space charge sign inversion (SCSI), or "type inversion" in conventional term, the sign of the space charge is negative at 300 K, as shown in Fig. 7 with hole current shapes. Trapping and subsequent freezing-out of free holes in neutron irradiation induced deep levels causes the sign of the space charge transforming from negative to positive (or SCT(-,+)) at around T=140 K. Same current shape degradation as that in the case of SCT(+,-) at lower temperatures due to partial depletion has been observed.

Fig. 8 shows the trapping induced SCT for detectors neutron irradiated to various fluences. It is clear that electron trapping causes space charge changing toward negative direction and the effect of hole trapping is just the opposite. The characteristic temperature T_C for electron trapping induced SCT is about 155 K, indicating an electron trap level at E_C-

0.4 eV. There are two levels for hole trapping induced SCT at 185 K and (E_v+0.48 eV) and 138 K (E_v+0.35 eV), respectively. The effect of free carrier trapping induced SCT is summarized in Table II.

It is obvious (from eq. (8)) that one may obtain the information of defect carrier capture cross section σ_t by measuring trapping time τ_t as a function of average injected free carrier concentration n_0. Various value of n_0 can be obtained by changing the laser repetition rate f [6]:

$$n_0 = \frac{Q_0}{e} \cdot t_{dr} \cdot \frac{f}{\lambda \cdot A} \qquad (10)$$

where t_{dr} is the average carrier drift time (about 10 ns (140 K, 100 V) for electrons), λ the laser absorption length (about 5 μm), and A the area of laser illumination (about 1 mm dia. spot). The measurement of is realised in a series of transient measurements of fast charge component (integrating current over $0 \le t \cong t_{dr}$) in a measurement time period (decay time) of $0 \le \tau_m \le 10\tau_t << \tau_d$. A large τ_d can be reached by making the measurements at lower temperature than T_c.

In a real transient measurement, the detector was biased at given bias and cooled from 300 K to a given low temperature T_m (140 K for electron injection and 125 K for hole injection). The laser was off during the cooling and was tuned on at t = 0 when T_m is reached and stabilised. Current shapes were measured during the decay period $t > 0$. Fig. 9 shows the transient measure data (electron trapping) of an irradiated detector. At f = 10 Hz, the time constant for the observed SCT(+,-) is about 60 second. The time constant was shortened by about a factor of 10 (about 6 seconds) when the frequency was increased by a factor of 10 to 100 Hz (Fig. 10), in agreement with eq. (8) and (10). The same trend listed in Table II also exists for transient SCT, i.e. no SCT for un-irradiated detectors and hole trapping causes SCR(-,+), etc. Fast component of the charge collected (Q) was obtained by integrating the current shape in a fixed time interval that is just a little bit longer than t_{dr} (20 ns in our case for Fig. 9 and 10). Normalized fast charge component (Q/Q_0) as a function of decay time for both electrons and holes are shown in Fig. 11. The trapping time constant τ_t is determined by the measurement of the time at which Q/Q_0 drops to its half

maximum ($\tau_{1/2}$). Only one τ_t can be identified in the case of electron trapping and two τ_t 's may be assigned for the case of hole trapping. When plotted in Fig. 12 as a function of n_0, the slopes of the straight lines give the carrier capture cross section of N_{eff} defects. Table III lists the (E_a, σ_t) parameter pairs for one electron trap level and two hole traps obtained from TCT. The parameters for the electron trap level (E_c -0.4 eV, 3.1×10^{-15} cm^2) is the same as those for the singly charged di-vacancy ($V\text{-}V^-$). The hole trap level with parameters (E_v +0.35 eV, 9.5×10^{-14} cm^2) should be the complex of interstitial carbon and interstitial oxygen ($C_i\text{-}O_i$) [8]. The identity of the hole trap level near the mid-bandgap (E_v +0.48 eV, 8.3×10^{-15} cm^2) is not yet known.

V. CONCLUSION

It has been shown in this study that N_{eff} defects can be measured directly using the TCT at various temperatures. Trapping of free electrons by one electron level, the $V\text{-}V^-$ center, has been identified as the cause for N_{eff} changes towards negative direction (SCT(++,+), SCT(+,-), and SCT(-,--)). This finding is also consistent with DLTS/TSC identification of a deep level with activation energy of about 0.4 eV being the one responsible for the reverse annealing effect (which is also a change of N_{eff} towards negative direction) at RT and elevated temperatures [9-10]. Trapping of free holes by two hole levels, the $C_i\text{-}O_i$ center and a deeper level that is unknown at this point, has been identified as the cause for N_{eff} changes towards positive direction (SCT(--,-), SCT(-,+), and SCT(+,++)). The carrier capture cross section for each deep level can also be measured independently using TCT. The degree of the N_{eff} transformation may also be as a quantitative determination of the concentration of N_{eff} defects (N_t). With some system modifications and modelling improvements, it is now possible to develop the Space Charge Transformation Spectroscopy (SCTS) as a direct tool to measure the complete set of parameters (N_t, E_a, σ_t) for N_{eff} defects.

REFERENCE

1. H.W. Kraner, Z. Li, and E. Fretwurst, Nucl. Instr. Meth., A326, 350(1993).
2. Z. Li, V. Eremin, N. Strokan, and E. Verbitskaya, IEEE Trans. Nucl. Sci., NS-239, No. 6, 1730(1992).
3. V. Eremin and Z. Li, IEEE Trans. Nucl. Sci., NS-41, No. 6, 1907(1994).
4. V. Eremin, N. Strokan, and E. Verbitskaya, and Z. Li, to be published in Nucl. Instr. Meth., (1996), in press.
5. V. Eremin and Z. Li, Nucl. Instr. Meth., A362, 338(1995).
6. V. Eremin, Z. Li, and I. Ijashenko, Nucl. Instr. Meth., A360, 458(1995).
7. Z. Li and H.W. Kraner, Nucl. Phys. B, Vol. 32, 398(1993).
8. V. Eremin, A. Ivanov, E. Verbitskaya, Z. Li, and H.W. Kraner, IEEE Trans. Nucl. Sci., Vol. 42, No.4, 387(1995).
9. Z. Li, C.J. Li, V. Eremin, and E. Verbitskaya, to be published in Nucl. Instr. Meth. (1996), in press.
10. U. Biggeri, et al., Nucl Phys. B, Vol. 44, 488(1995).

Figure Captions

Fig. 1 Schematic of the BNL's TCT set-up.

Fig. 2 Schematics of the electric field distribution of a $p^+/n/n^+$ silicon detector: a) field distribution before SCSI (JF); b) field distribution after SCSI (JB).

Fig. 3 Simulated hole current shapes (JBLB) with various values of N_{eff}.

Fig. 4 Simulated current shapes and dependence of the top slope S on temperature: a) electron current shapes; b) hole current shapes.

Fig. 5 Measured steady-state current shapes at various temperatures for an un-irradiated detector: a) electron current shapes; b) hole current shapes.

Fig. 6 Measured steady-state current shapes at various temperatures for an irradiated detector (before SCSI): a) electron current shapes; b) hole current shapes.

Fig. 7 Measured steady-state current shapes at various temperatures for an irradiated detector (after SCSI): a) electron current shapes; b) hole current shapes.

Fig. 8 Free carrier trapping induced N_{eff} transformation for detectors irradiated to various n-fluences: a) low fluence; b) medium fluence; and c) high fluence.

Fig. 9 Measured transient electron current shapes at various decay time and at $f = 10$ Hz for an irradiated detector.

Fig. 10 Measured transient electron current shapes at various decay time and at $f = 100$ Hz for an irradiated detector.

Fig. 11 Plot of normallized fast charge component as a function of decay time with laser period ($1/f$) as a parameter.

Fig. 12 Plots of trapping time constants as a function of average free carrier concentration forvarious defect levels.

Tables

Table I Measured low field drift mobility for holes at various temperatures[5]

T (K)	110	170	200	250	274	300
μ_0^e (cm/V/s)	14400	9000	5900	4150	1928	1590
μ_0^h (cm/V/s)	4800	3150	2180	813	635	507

Table II Summary of free carrier trapping induced N_{eff} transformations (or SCT) by radiation induced defects in high resistivity silicon detectors

n-fluence (n/cm^2)	N_{eff} Sign at RT	e-trapping (155 K)	h-trapping (185 K and 138 K)
0	+	None	None
Low ($<10^{12}$)	+	SCT(+, ~0)	SCT(+,++)
Medium (10^{12} to 10^{13})	+ to 0	SCT(+,-)	SCT(+,++)
High ($>10^{13}$)	-	SCT(-,--)	SCT(-,+)

Table III Defect parameters measured by TCT

T_C (K)	Energy level	Cross section (cm^2)	ID
138	E_V+0.35 eV	$9.5x10^{-14}$ cm^2	$V\text{-}V^-$
155	E_C -0.4 eV	$3.1x10^{-15}$ cm^2	$C_i\text{-}O_i$
185	E_V+0.48 eV	$8.3x10^{-15}$ cm^2	? V_3O?

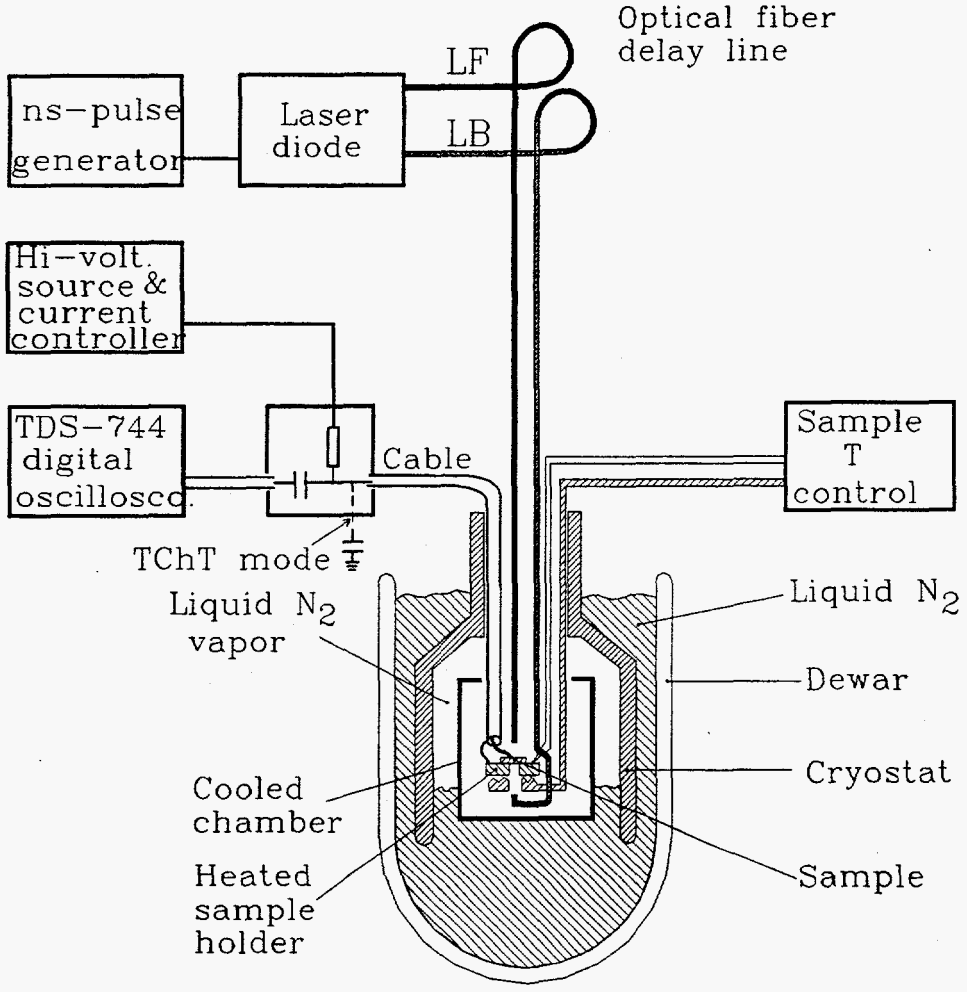

TCT/TChT

Fig. 1

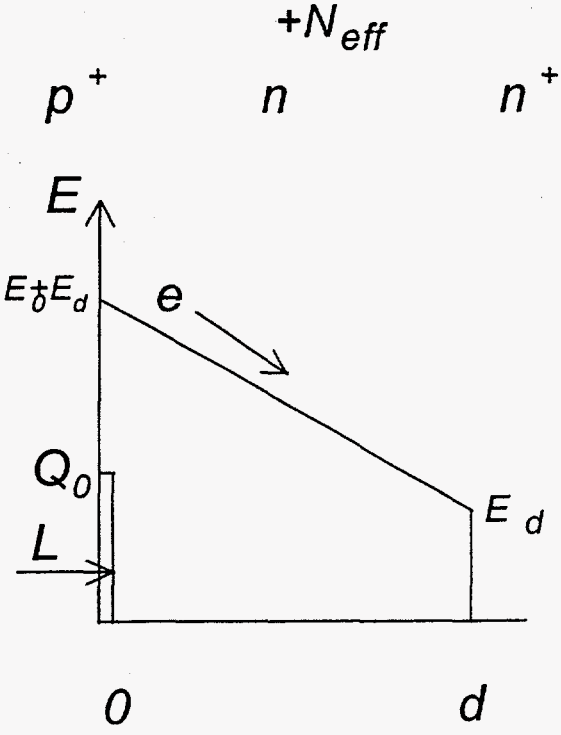

a)

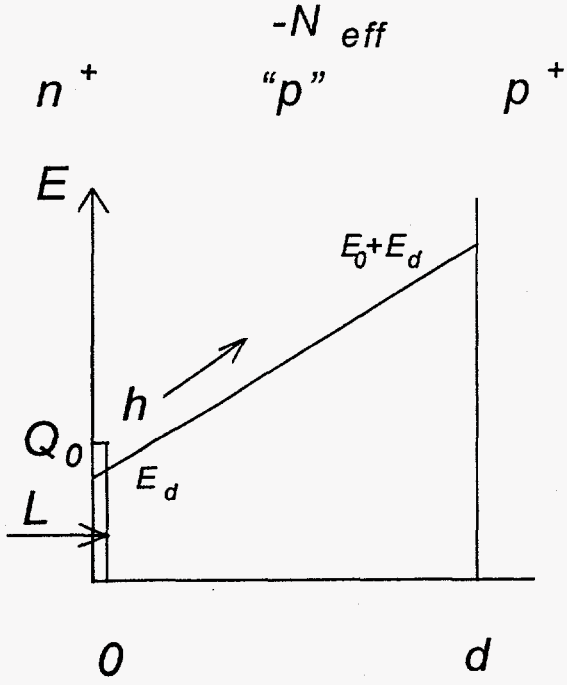

b)

Fig. 2

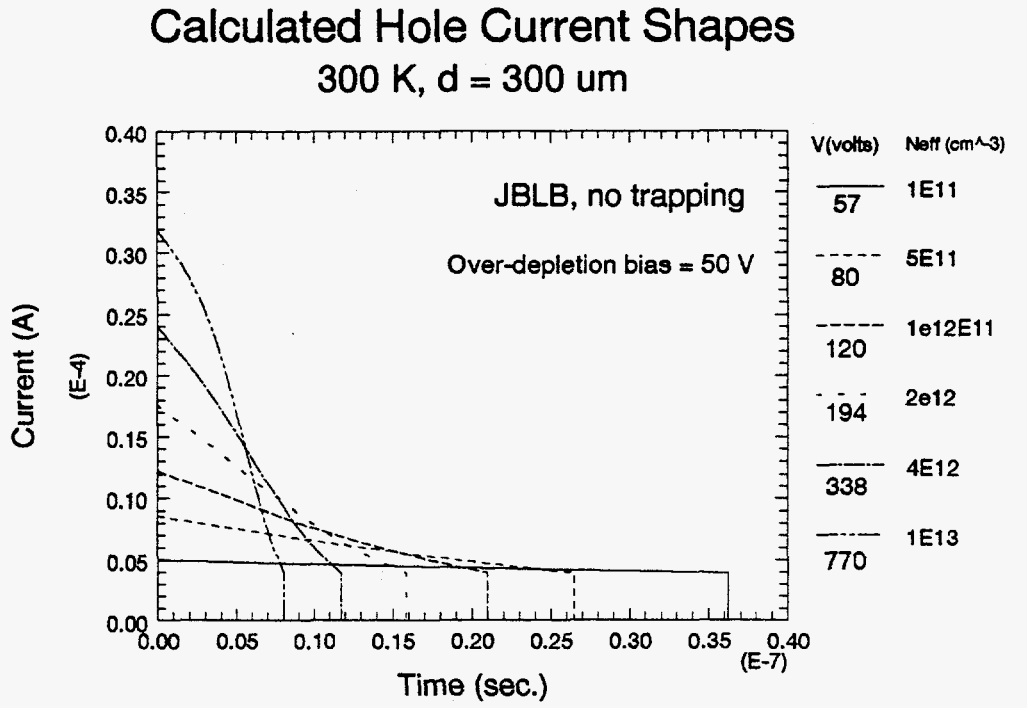
Calculated Hole Current Shapes
300 K, d = 300 um
JBLB, no trapping
Over-depletion bias = 50 V
V(volts)
Neff (cm^-3)
57
1E11
80
5E11
120
1e12E11
194
2e12
338
4E12
770
1E13
Current (A)
(E-4)
Time (sec.)
(E-7)
0.00
0.05
0.10
0.15
0.20
0.25
0.30
0.35
0.40
429-33 A : Fig10.tc

a)

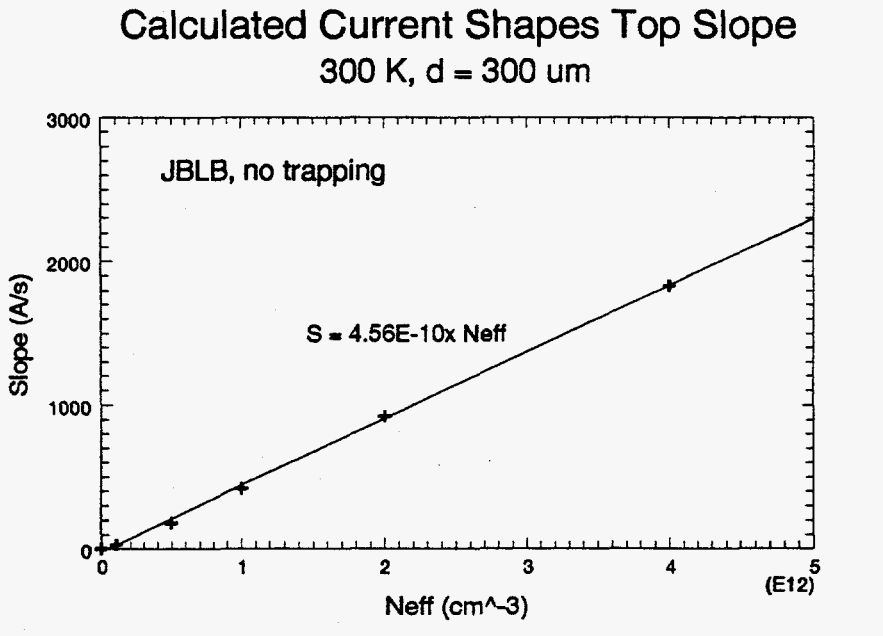
Calculated Current Shapes Top Slope
300 K, d = 300 um
JBLB, no trapping
S = 4.56E-10x Neff
Slope (A/s)
Neff (cm^-3)
(E12)
0
1000
2000
3000
1
2
3
4
5
429-33 A : Fig11.tc

b)

Fig.3

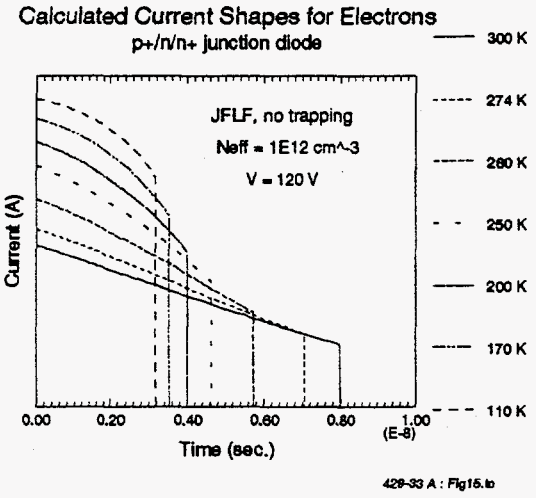
Calculated Current Shapes for Electrons
p+/n/n+ junction diode
JFLF, no trapping
Neff = 1E12 cm^-3
V = 120 V
300 K
274 K
260 K
250 K
200 K
170 K
110 K
Current (A)
0.00
0.20
0.40
0.60
0.80
1.00
(E-8)
Time (sec.)
429-33 A : Fig15.tc

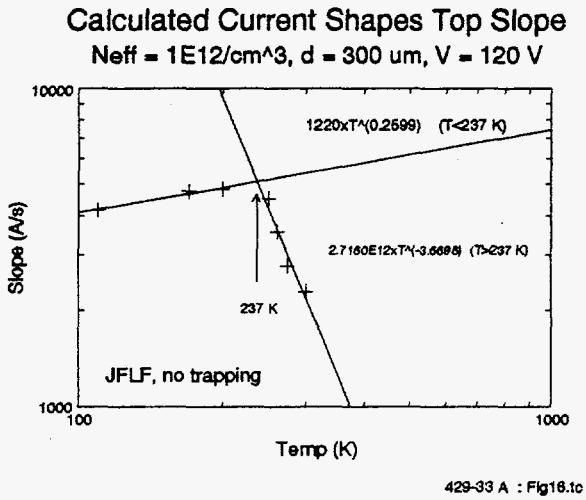
Calculated Current Shapes Top Slope
Neff = 1E12/cm^3, d = 300 um, V = 120 V
1220xT^(0.2599) (T<237 K)
2.7160E12xT^(-3.6698) (T>237 K)
237 K
JFLF, no trapping
Slope (A/s)
10000
1000
100
1000
Temp (K)
429-33 A : Fig16.tc

a)

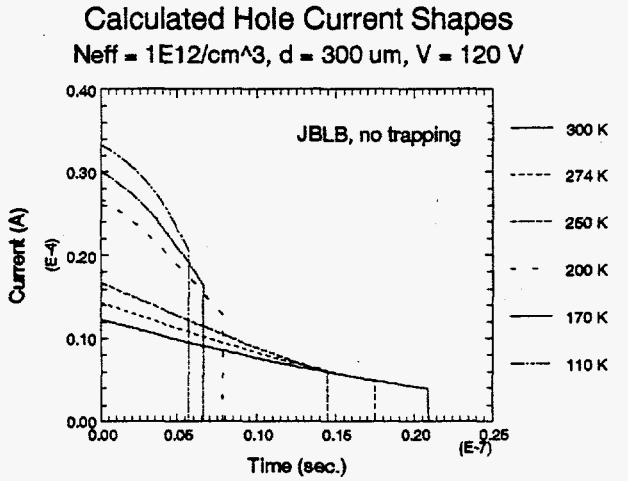
Calculated Hole Current Shapes
Neff = 1E12/cm^3, d = 300 um, V = 120 V
JBLB, no trapping
300 K
274 K
250 K
200 K
170 K
110 K
Current (A)
(E-4)
0.40
0.30
0.20
0.10
0.00
0.00
0.05
0.10
0.15
0.20
0.25
(E-7)
Time (sec.)
429-33 A : Fig7.tc

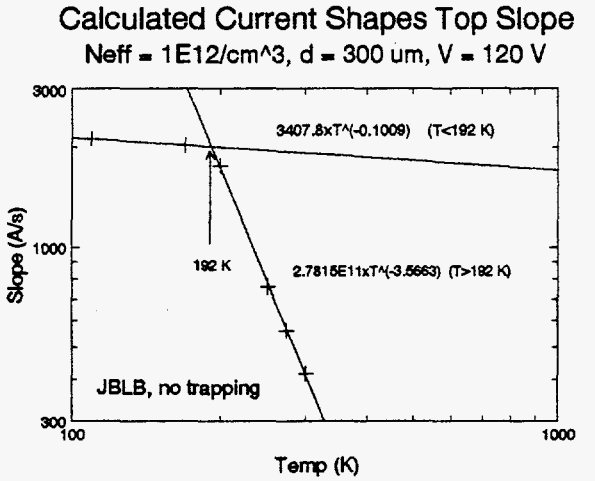
Calculated Current Shapes Top Slope
Neff = 1E12/cm^3, d = 300 um, V = 120 V
3407.8xT^(-0.1009) (T<192 K)
192 K
2.7815E11xT^(-3.5663) (T>192 K)
JBLB, no trapping
Slope (A/s)
3000
1000
300
100
1000
Temp (K)
429-33 A : Fig9.tc

b)

Fig. 4

#NO6-121, n(111) 12 K Ω-cm, 368 μm, no radiation
V=70 volts

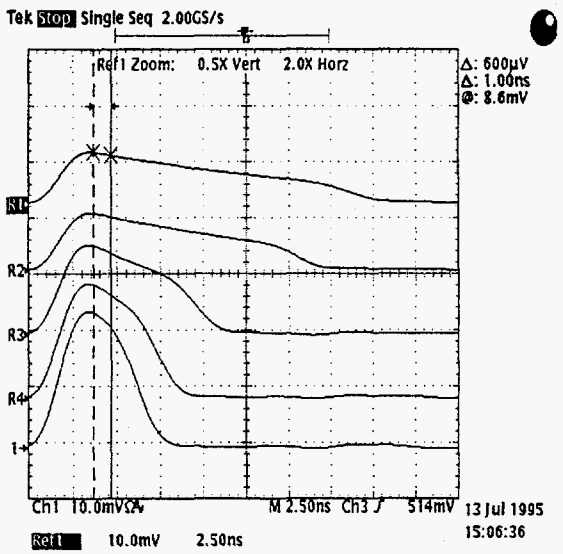

a) Electron current shapes at temps: R1: 300 K; R2: 274 K; R3: 200 K; R4: 110 K

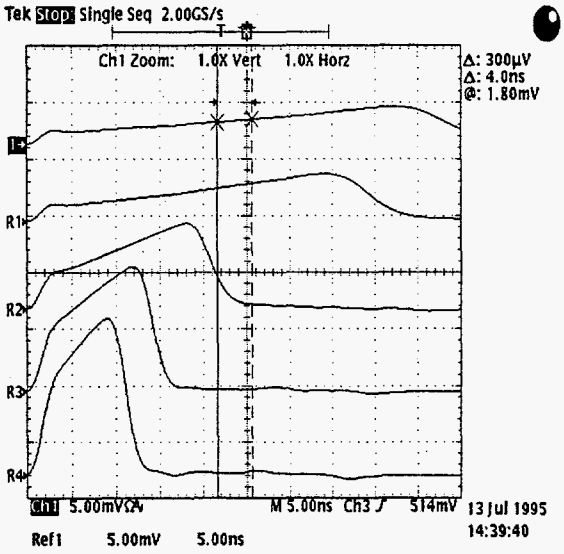

b)Hole current shapes at temps: 1: 300 K; R1: 274 K; R2: 200 K; R3: 150 K; R4: 110 K

Fig. 5

Trapping Induced Neff Transformation

#296-A3, 4k, 630 μm, 0.25 cm^2, laser (670 nm) on the p^+ side (electron trapping)

2.3x10^{12} n/cm^2, 31-month RTA, V = 100 V

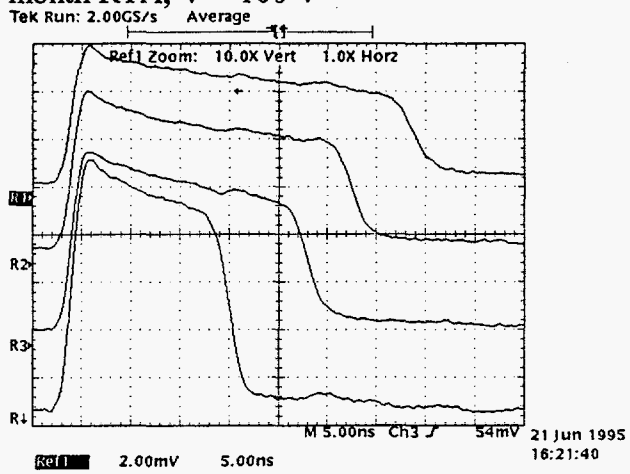

a) R1: 300K; R2: 274K; R3: 250K; R4: 200K

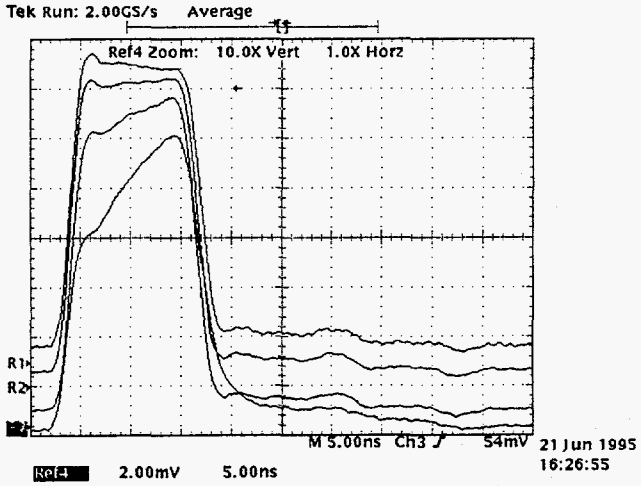

b) R1: 170K; R2: 165K; R3: 160K; R4: 155K

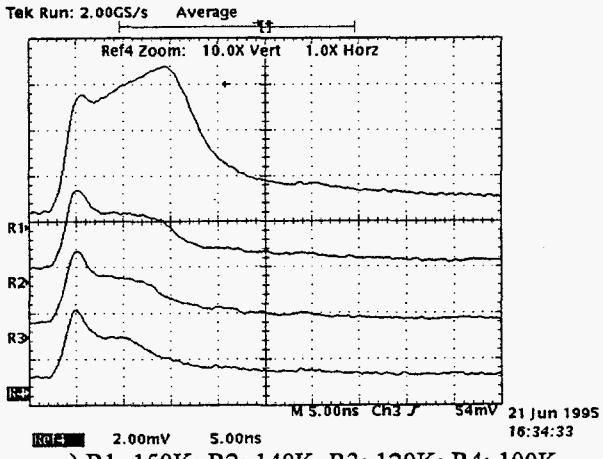

c) R1: 150K; R2: 140K; R3: 120K; R4: 100K

Fig. 6

Trapping Induced Neff Transformation

#296-B14, 4k, 630 μm, 0.25 cm^2, laser (832 nm) on the n^+ side (hole trapping)

1.02x10^{13} n/cm^2, 33-month RTA

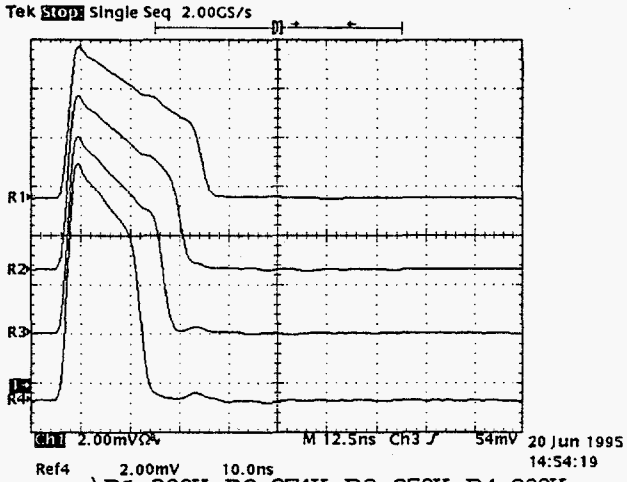

a) R1:300K ; R2:274K ; R3:250K ; R4:200K

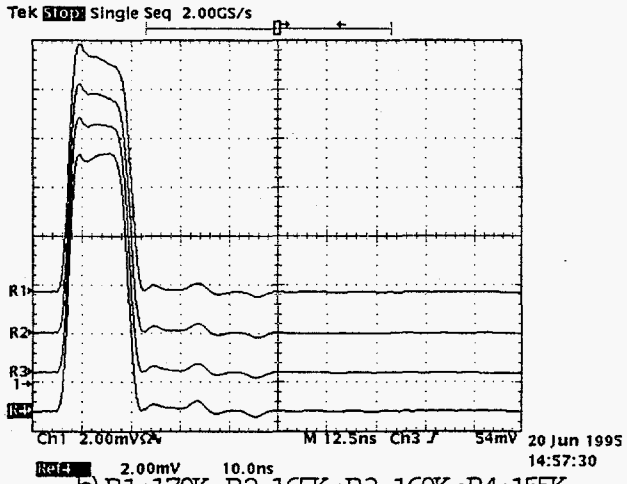

b) R1:170K ; R2:165K ; R3:160K ; R4:155K

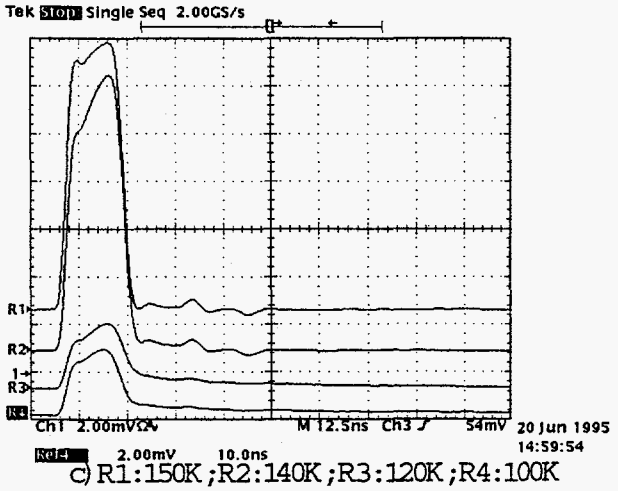

c) R1:150K ; R2:140K ; R3:120K ; R4:100K

296 A : Fig1.doc

Fig. 7

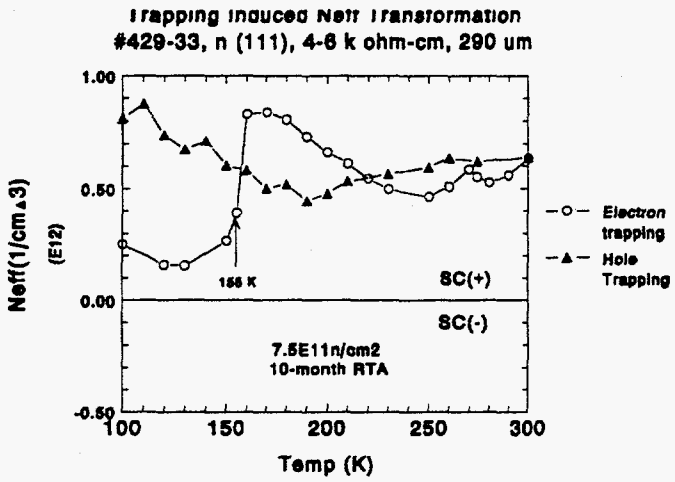
Trapping Induced Neff Transformation
#429-33, n (111), 4-6 k ohm-cm, 290 um
Neff(1/cm^3)
(E12)
1.00
0.50
0.00
-0.50
156 K
SC(+)
SC(-)
7.5E11n/cm2
10-month RTA
100
150
200
250
300
Temp (K)
Electron trapping
Hole Trapping
429-33 A: Fig1.tc

a)

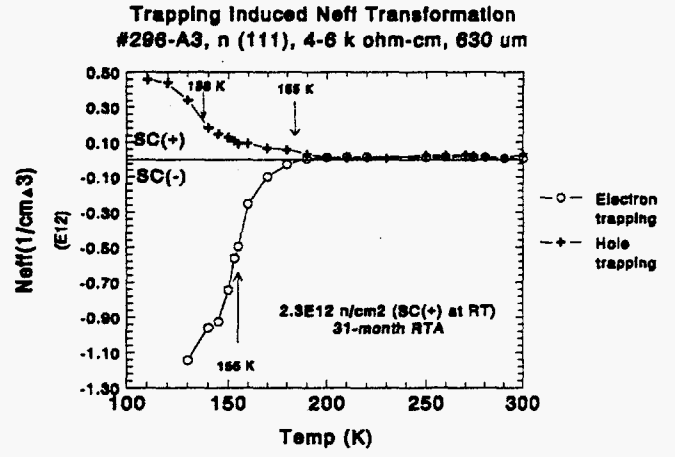
Trapping Induced Neff Transformation
#296-A3, n (111), 4-6 k ohm-cm, 630 um
Neff(1/cm^3)
(E12)
0.50
0.30
0.10
-0.10
-0.30
-0.50
-0.70
-0.90
-1.10
-1.30
156 K
155 K
SC(+)
SC(-)
2.3E12 n/cm2 (SC(+) at RT)
31-month RTA
100
150
200
250
300
Temp (K)
Electron trapping
Hole trapping
429-33 A: Fig2.tc

b)

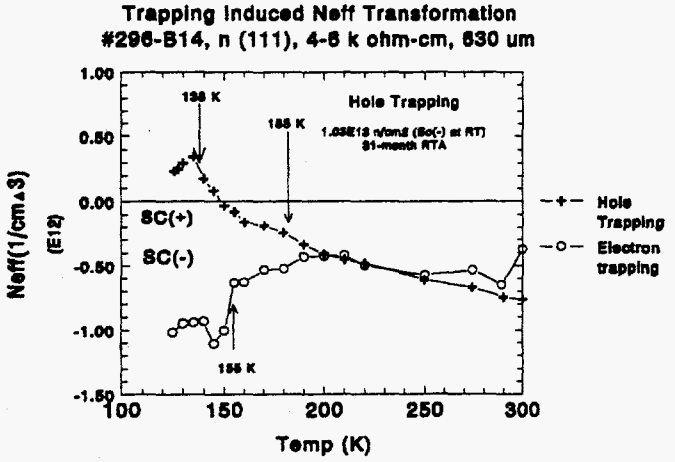
Trapping Induced Neff Transformation
#296-B14, n (111), 4-6 k ohm-cm, 630 um
Neff(1/cm^3)
(E12)
1.00
0.50
0.00
-0.50
-1.00
-1.50
156 K
155 K
Hole Trapping
SC(+)
SC(-)
100
150
200
250
300
Temp (K)
Hole Trapping
Electron trapping
429-33 A: Fig4.tc

c)

Fig. 8

Trapping Induced Neff Transformation

#296-A3, 4k, 630 μm, 0.25 cm^2, laser (670 nm) on the p^+ side (electron trapping)

$2.3x10^{12}$ n/cm^2, 31-month RTA, V = 100 volts, T = 140 K

t = 100 ms (f = 10 Hz, or $n_0 = 8.185x10^3$ $/cm^3$)

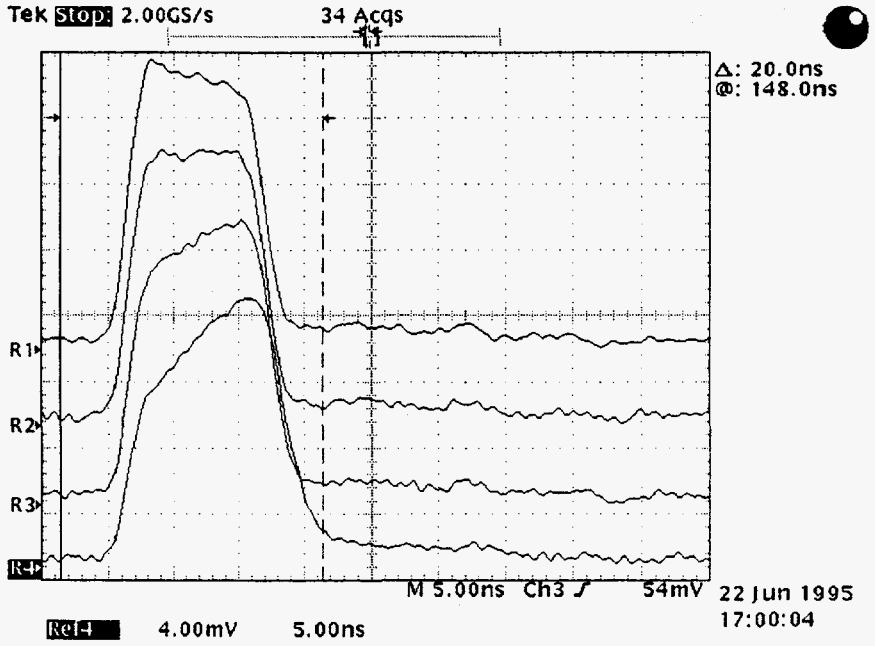

a) Decay time(sec): R1: 5; R2: 60; R3: 240; R4: 540

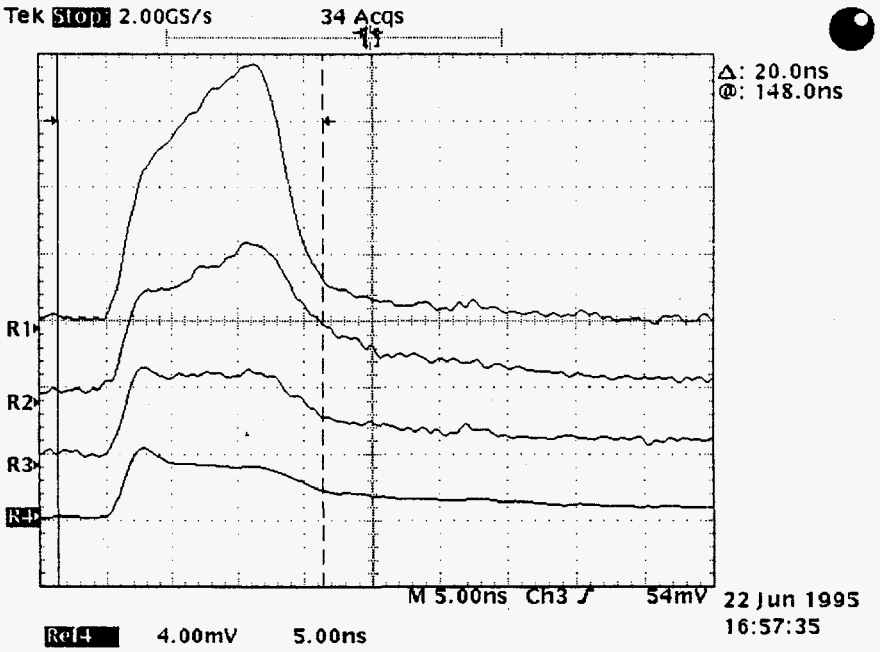

b) Decay time(min.): R1: 10; R2: 18; R3: 30; R4: 60

296 I: Fig8.doc

Fig. 9

Trapping Induced Neff Transformation

#296-A3, 4k, 630 μm, 0.25 cm^2, laser (670 nm) on the p^+ side (electron trapping)

$2.3x10^{12}$ n/cm^2, 31-month RTA, V = 100 volts, T = 140 K

t = 10 ms (f = 100 Hz, or $n_0 = 8.185x10^4$ $/cm^3$)

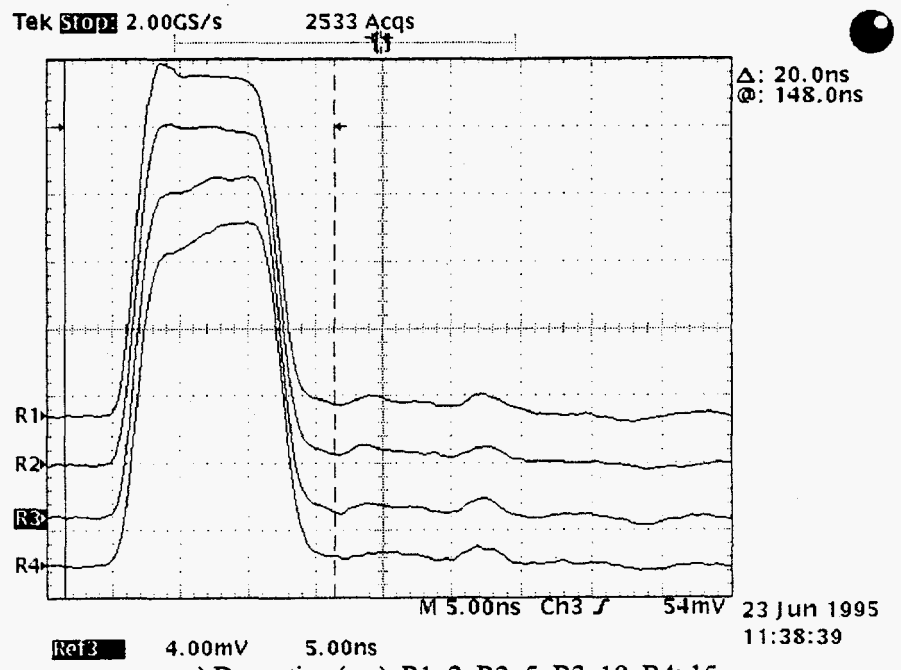

a) Decay time(sec): R1: 2; R2: 5; R3: 10; R4: 15

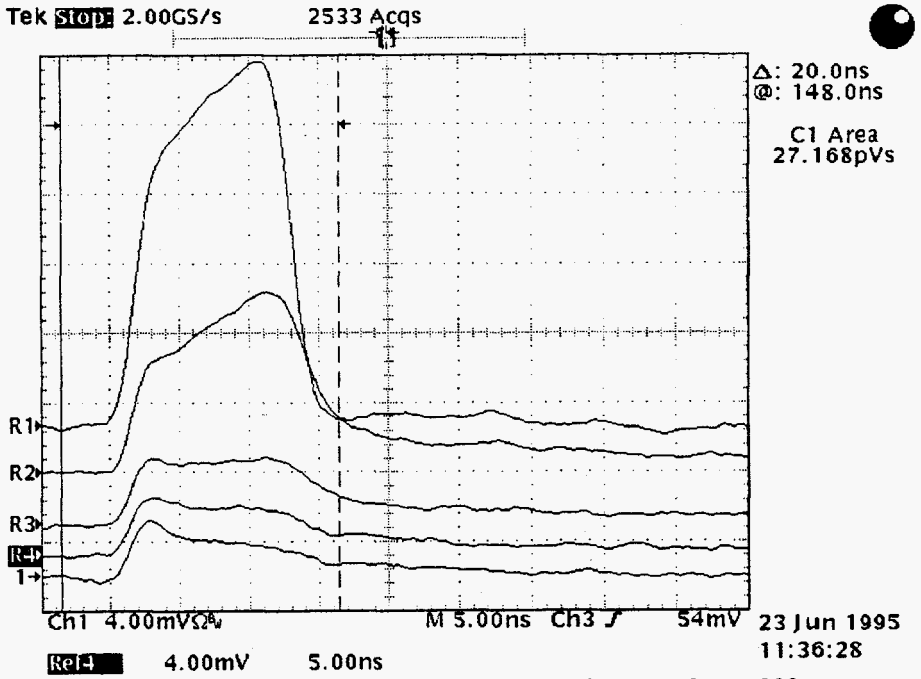

a) Decay time(sec.): R1: 30; R2: 60; R3: 105; R4: 135; 1: 300

Fig. 10

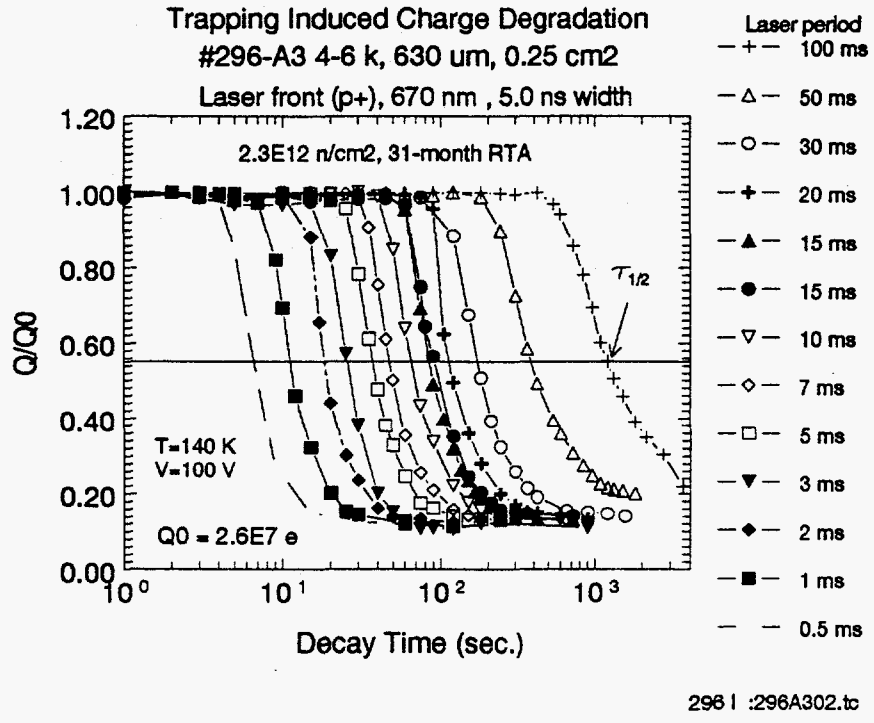
Trapping Induced Charge Degradation
#296-A3 4-6 k, 630 um, 0.25 cm2
Laser front (p+), 670 nm , 5.0 ns width
2.3E12 n/cm2, 31-month RTA
T=140 K
V=100 V
Q0 = 2.6E7 e
τ1/2
Q/Q0
Decay Time (sec.)
Laser period
100 ms
50 ms
30 ms
20 ms
15 ms
15 ms
10 ms
7 ms
5 ms
3 ms
2 ms
1 ms
0.5 ms
296 l :296A302.tc

a)

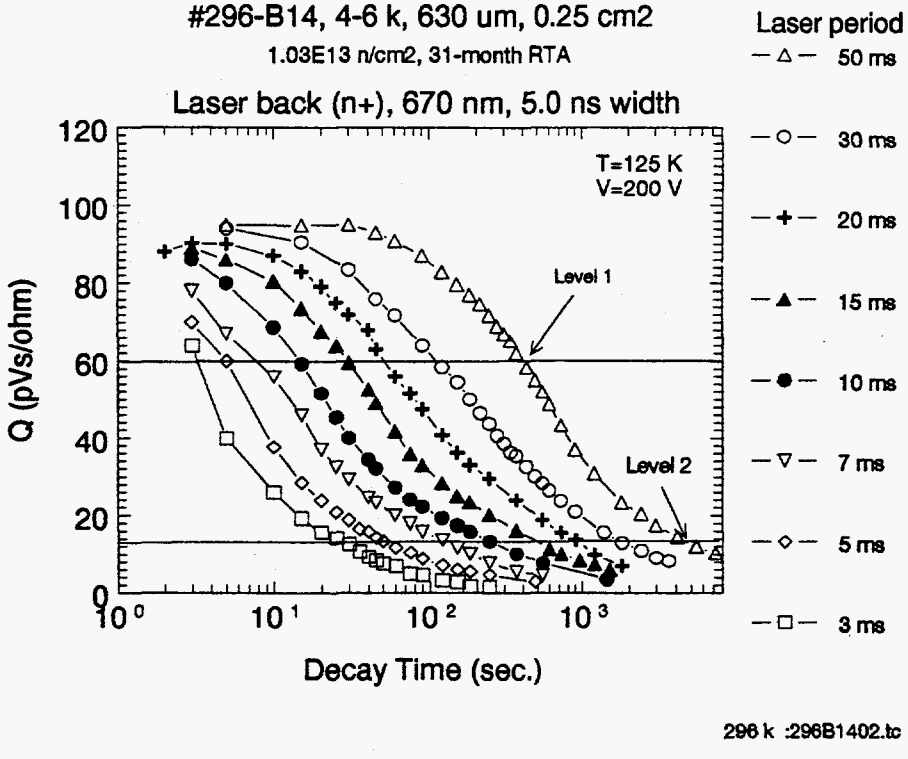
#296-B14, 4-6 k, 630 um, 0.25 cm2
1.03E13 n/cm2, 31-month RTA
Laser back (n+), 670 nm, 5.0 ns width
T=125 K
V=200 V
Level 1
Level 2
Q (pVs/ohm)
Decay Time (sec.)
Laser period
50 ms
30 ms
20 ms
15 ms
10 ms
7 ms
5 ms
3 ms
296 k :296B1402.tc

b)

Fig. 11

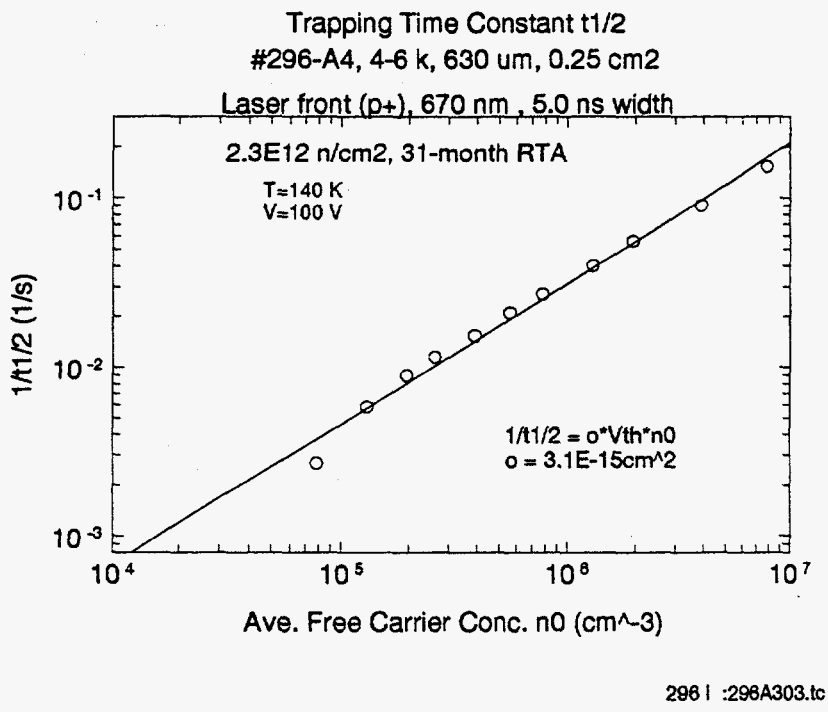
Trapping Time Constant t1/2
#296-A4, 4-6 k, 630 um, 0.25 cm2
Laser front (p+), 670 nm , 5.0 ns width
2.3E12 n/cm2, 31-month RTA
T=140 K
V=100 V
1/t1/2 = o*Vth*n0
o = 3.1E-15cm^2
1/t1/2 (1/s)
Ave. Free Carrier Conc. n0 (cm^-3)
296 I :296A303.tc

a)

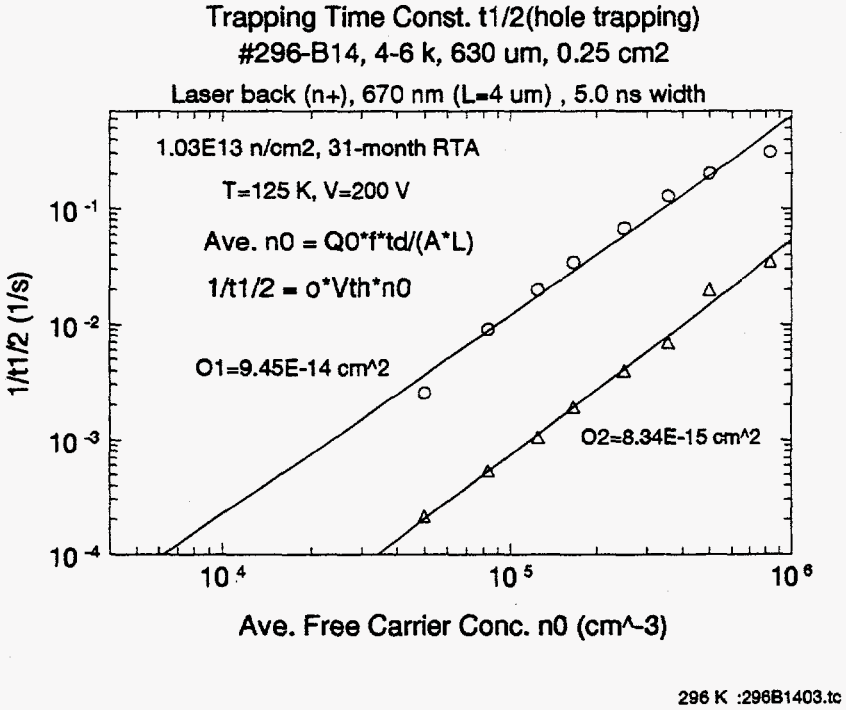
Trapping Time Const. t1/2(hole trapping)
#296-B14, 4-6 k, 630 um, 0.25 cm2
Laser back (n+), 670 nm (L=4 um) , 5.0 ns width
1.03E13 n/cm2, 31-month RTA
T=125 K, V=200 V
Ave. n0 = Q0*f*td/(A*L)
1/t1/2 = o*Vth*n0
O1=9.45E-14 cm^2
O2=8.34E-15 cm^2
1/t1/2 (1/s)
Ave. Free Carrier Conc. n0 (cm^-3)
296 K :296B1403.tc

b)

Fig. 12

DISCLAIMER